# Molecular Determinants of the Binding Specificity of BH3 Ligands to BclXL Apoptotic Repressor

Vikas Bhat, Max B. Olenick, Brett J. Schuchardt, David C. Mikles, Caleb B. McDonald, Amjad Farooq

*Department of Biochemistry and Molecular Biology, Miller School of Medicine, University of Miami, Miami, FL 33136*

*Received 19 June 2013; revised 22 September 2013; accepted 23 September 2013*
*Published online 3 October 2013 in Wiley Online Library (wileyonlinelibrary.com). DOI 10.1002/bip.22419*

## ABSTRACT:

*B-cell lymphoma extra-large protein (BclXL) serves as an apoptotic repressor by virtue of its ability to recognize and bind to BH3 domains found within a diverse array of proapoptotic regulators. Herein, we investigate the molecular basis of the specificity of the binding of proapoptotic BH3 ligands to BclXL. Our data reveal that while the BH3 ligands harboring the LXXX[A/S]D and [R/Q]XLXXXGD motif bind to BclXL with high affinity in the submicromolar range, those with the LXXXGD motif afford weak interactions. This suggests that the presence of a glycine at the fourth position (G+4)—relative to the N-terminal leucine (L0) within the LXXXGD motif—mitigates binding, unless the LXXXGD motif also contains arginine/glutamine at the −2 position. Of particular note is the observation that the residues at the +4 and −2 positions within the LXXX[A/S]D and [R/Q]XLXXXGD motifs appear to be energetically coupled—replacement of either [A/S]+4 or [R/Q]-2 with other residues has little bearing on the binding affinity of BH3 ligands harboring one of these motifs. Collectively, our study lends new molecular insights into understanding the binding specificity of BH3 ligands to BclXL with important consequences on the design of novel anticancer drugs.*

*Biopolymers 101: 573–582, 2014.*

*Keywords: BclXL-BH3 recognition; binding specificity; salt dependence; energetic coupling*

*This article was originally published online as an accepted preprint. The "Published Online" date corresponds to the preprint version. You can request a copy of the preprint by emailing the Biopolymers editorial office at biopolymers@wiley.com*

## INTRODUCTION

The B-cell lymphoma extra-large protein (BclXL) apoptotic repressor belongs to the B-cell lymphoma protein 2 (Bcl2) family of proteins that play a central role in determining the apoptotic fate of cells during physiological processes such as embryonic development and cellular homeostasis.[1–8] Briefly, the Bcl2 proteins can be divided into three major groups with respect to their role in the regulation of apoptotic machinery: activators, effectors and repressors (Figure 1a). In a nutshell, the apoptotic fate—or the decision of a cell to live or die—is determined by the cellular ratio of activator, effector and repressor molecules.[9,10] In quiescent and healthy cells, the effectors such as Bcl2-associated protein X (Bax) and Bcl2-homologous antagonist/killer (Bak) are maintained in an inactive state via complexation with repressors such as BclXL and Bcl2. Upon receiving apoptotic cues, in the form of DNA damage and cellular stress, the activators such as BH3-interacting domain death agonist (Bid) and Bcl2-associated death promoter (Bad) are stimulated and compete with

*Correspondence to:* Amjad Farooq; e-mail: amjad@farooqlab.net
Contract grant sponsor: National Institutes of Health
Contract grant number: R01-GM083897 T32-CA119929
Contract grant sponsor: USylvester Braman Family Breast Cancer Institute (to A.F.).

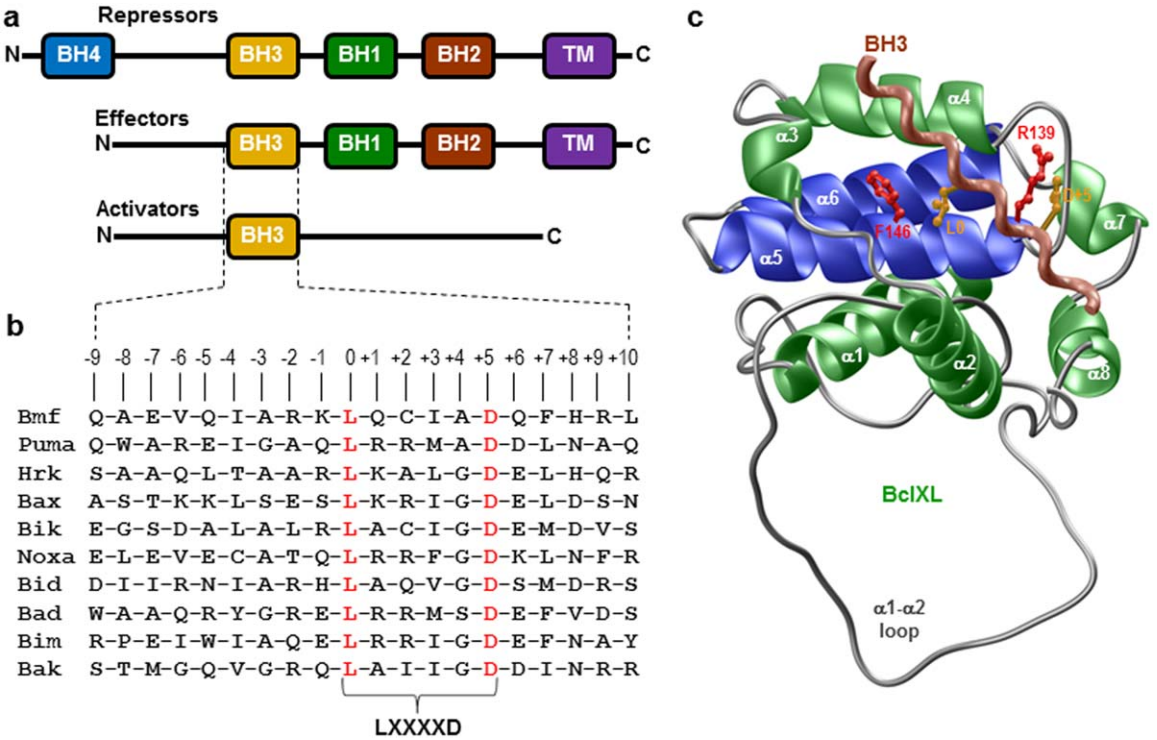


**FIGURE 1** An overview of Bcl2 proteins. (a) Modular organization of repressors, effectors, and activators. The activators belong to the BH3-only proteins, where BH3 is the Bcl2 homology 3 domain. Examples of activators include Bad, Bid, Bik, Bim, Bmf, Hrk, Noxa, and Puma. The effectors contain the BH3-BH1-BH2-TM modular architecture, where TM is the transmembrane domain located C-terminal to Bcl2 homology domains BH3, BH1, and BH2. Examples of effectors are Bak and Bax. The repressors are usually characterized by the BH4-BH3-BH1-BH2-TM modular organization, with an additional N-terminal Bcl2 homology 4 domain. Examples of repressors are BclXL, Bcl2, Bcl2-like protein 2 (BclW), myeloid leukemia cell protein 1 (Mcl1), and Bcl2-related protein A1 (Bfl1). (b) Amino acid sequence alignment of BH3 domains of various effectors and activators encoded by the human genome and employed in this study as ligands for BclXL. Note that the absolutely conserved consensus leucine and aspartate residues within the core LXXXXD motif shared by all BH3 domains are colored red. The numerals indicate the nomenclature used in this study to distinguish residues within and flanking the core LXXXXD motif relative to the consensus leucine, which is arbitrarily assigned zero. (c) Structural model of BclXL bound to BH3 peptide of Puma. In BclXL, the hydrophobic α-helical hairpin dagger (α5/α6) is colored blue, the amphipathic α-helical cloak (α1–α4 and α7–α8) is colored green, and the loops in gray. The C-terminal TM domain (α9 helix) was not modeled into the structure for the sake of simplicity. The α-helical BH3 peptide is colored brown. Note that the consensus leucine (L0) and aspartate (D+5) residues within the LXXXXD motif of BH3 peptide are shown in yellow and their respective intermolecular counterparts (F146 and R139) within BclXL in red.

effectors for binding to the repressors and, in so doing, not only do they neutralize the antiapoptotic action of repressors but also unleash the proapoptogenicity of effectors. The effectors subsequently initiate apoptotic cell death by virtue of their ability to insert into the mitochondrial outer membrane (MOM) resulting in the formation of mitochondrial pores in a manner akin to the insertion of bacterial toxins such as colicins and diphtheria.[11–15] This leads to the release of apoptogenic factors such as cytochrome c and Smac/Diablo from mitochondria into the cytosol. Subsequently, rising levels of apoptogenic factors in the cytosol switch on aspartate-specific proteases termed caspases, which in turn, demolish the cellular architecture by cleavage of proteins culminating in total cellular destruction. In this manner, the concerted action of various Bcl2 proteins keeps apoptosis in check in an healthy cell, while their dysregulation is met with serious pathological consequences. In particular, overexpression of BclXL and Bcl2 apoptotic repressors is associated

with the development of various cancers.[16–18] Tellingly, BclXL and Bcl2 rank among some of the most attractive targets for anticancer therapy.

While there is a general consensus that hetero-association between various members of the Bcl2 family represents a defining event in the decision of a cell to live or die, the molecular basis of such protein–protein interactions remains hitherto poorly characterized. In particular, the BH3 domain of activators and effectors—which is typically about 20 amino acids in length and characterized by the presence of the core LXXXXD motif (Figure 1b)—has risen to prominence for its key role in mediating apoptosis on at least two major fronts. First, the repressors unleash their antiapoptotic action by virtue of their ability to bind to the BH3 domain of effectors. Second, the activators initiate apoptosis by virtue of the ability of their BH3 domains to compete with the BH3 domains of effectors for binding to repressors and, in so doing, drive the apoptotic machinery by neutralizing the repressors. While substantial efforts have been made over the past decade or so in understanding the molecular basis of the binding specificity of BH3 domains of activators and effectors to apoptotic repressors,[19–31] further work is clearly warranted. Toward this goal, we employ here various biophysical tools to investigate the molecular basis of the specificity of the binding of proapoptotic BH3 ligands to BclXL apoptotic repressor. Briefly, on the basis of its known atomic structure alone and bound to various BH3 peptides,[19,21–23] BclXL is characterized by canonical Bcl2 topological fold harboring a central predominantly hydrophobic α-helical hairpin "dagger" (α5/α6) surrounded by a "cloak" comprised of six amphipathic α-helices (α1–α4 and α7–α8) of varying lengths (Figure 1c). Additionally, BclXL contains a C-terminal hydrophobic α-helix termed α9, or more commonly the transmembrane (TM) domain, which plays an important role in the localization of BclXL to MOM upon apoptotic induction.[32–34] Importantly, the BH3 peptides adopt an amphipathic α-helical conformation within the ligand binding groove—a shallow cleft formed by the juxtaposition of α2–α5 helices within BclXL—and are stabilized via numerous intermolecular contacts. It is noteworthy that while the consensus L0 and D+5 residues within the LXXXXD motif account for core intermolecular interactions between BH3 peptides and BclXL, residues within and flanking this motif further buttress these intermolecular contacts. In this study, we provide evidence that the various BH3 ligands can be dissected into three distinct classes harboring the LXXX[A/S]D, LXXXGD, and [R/Q]XLXXXGD motifs on the basis of their binding characteristics to BclXL. Our detailed biophysical analysis sheds new light on the mechanism of BclXL-ligand recognition.

## MATERIALS AND METHODS

### Sample Preparation

Human BclXL (residues 1–200) was cloned into pET30 bacterial expression vector with an N-terminal His-tag using Novagen ligation-independent cloning (LIC) technology, expressed in *Escherichia coli* BL21*(DE3) bacterial strain (Invitrogen) and purified on a Ni-NTA affinity column using standard procedures as described previously.[35,36] Protein concentration was determined by the fluorescence-based Quant-It assay (Invitrogen) and spectrophotometrically on the basis of an extinction coefficient of 41,940 $M^{-1}$ $cm^{-1}$ calculated using the online software ProtParam at ExPasy Server.[37] Results from both methods were in an excellent agreement. The 20-mer wildtype and mutant peptides spanning the BH3 domains from various human apoptotic effectors and activators were commercially obtained from GenScript Corporation. The amino acid sequence of wildtype BH3 peptides employed in this study is provided in Figure 1b. The concentration of all BH3 peptides was measured gravimetrically.

### Isothermal Titration Calorimetry

Isothermal titration calorimetry (ITC) experiments were performed on a Microcal VP-ITC instrument. Briefly, BclXL and various BH3 peptides were prepared in 50 m*M* sodium phosphate buffer containing 0–500 m*M* NaCl, 1 m*M* EDTA and 5 m*M* β-mercaptoethanol at pH 7.0. ITC experiments were initiated by injecting 25 × 10 μl aliquots of 1–4 m*M* of each BH3 peptide from the syringe into the calorimetric cell containing 50–100 μ*M* of 1.46 ml of BclXL at various temperatures in the 15–35°C range. In each case, the change in thermal power as a function of each injection was automatically recorded using the ORIGIN software and the raw data were further processed to yield binding isotherms of heat release per injection as a function of molar ratio of each BH3 peptide to BclXL. The heats of mixing and dilution were subtracted from the heats of binding per injection by carrying out a control experiment in which the same buffer in the calorimetric cell was titrated against each BH3 peptide in an identical manner. The apparent equilibrium dissociation constant ($K_d$) and the enthalpic change ($\Delta H$) associated with peptide binding to BclXL were determined from the nonlinear least-squares fit of data to a one-site model as described previously.[36,38] The binding free energy change ($\Delta G$) was calculated from the following expression:

$$\Delta G = RT \ln K_d \quad (1)$$

where $R$ is the universal molar gas constant (1.99 cal/K/mol) and $T$ is the absolute temperature. The entropic contribution ($T\Delta S$) to the free energy of binding was calculated from the relationship:

$$T\Delta S = \Delta H - \Delta G \quad (2)$$

where $\Delta H$ and $\Delta G$ are as defined above. Heat capacity change ($\Delta C_p$) and enthalpy change at 60°C ($\Delta H_{60}$) associated with peptide binding to BclXL were determined from the slopes and $y$-extrapolations to a temperature of 60°C of $\Delta H$–$T$ plots, respectively.

### SASA Calculations

Changes in solvent-accessible surface area (SASA) upon the binding of various BH3 peptides to BclXL were subsequently calculated from the experimentally determined values of $\Delta C_p$ and $\Delta H_{60}$. To determine

changes in polar SASA ($\Delta SASA_{polar}$) and apolar SASA ($\Delta SASA_{apolar}$) upon peptide binding to BclXL, it was assumed that $\Delta C_p$ and $\Delta H_{60}$ are additive and linearly depend on the change in $\Delta SASA_{polar}$ and $\Delta SASA_{apolar}$ as embodied in the following empirically derived expressions[39–42]:

$$\Delta C_p = a[\Delta SASA_{polar}] + b[\Delta SASA_{apolar}] \quad (3)$$

$$\Delta H_{60} = c[\Delta SASA_{polar}] + d[\Delta SASA_{apolar}] \quad (4)$$

where *a*, *b*, *c*, and *d* are empirically determined coefficients with values of −0.14 cal/mol/K/Å$^2$, +0.32 cal/mol/K/Å$^2$, +31.34 cal/mol/Å$^2$, and −8.44 cal/mol/Å$^2$, respectively. The coefficients *a* and *b* are independent of temperature, while *c* and *d* refer to a temperature of 60°C, which equates to the median melting temperature of the proteins from which these constants are derived.[39–42] With $\Delta C_p$ and $\Delta H_{60}$ experimentally determined using ITC and the knowledge of coefficients *a*–*d* from empirical models,[39–42] Eqs. (3) and (4) were simultaneously solved to obtain the magnitudes of $\Delta SASA_{polar}$ and $\Delta SASA_{apolar}$. Total change in SASA ($\Delta SASA_{total}$) is defined by the following equation:

$$\Delta SASA_{total} = \Delta SASA_{polar} + \Delta SASA_{apolar} \quad (5)$$

### Molecular Modeling

Structural model of BclXL (residues 1–200) in complex with 20-mer BH3 peptide derived from p53-upregulated modulator of apoptosis (Puma) was built using the MODELLER software based on homology modeling.[43] Briefly, the structural model was constructed using, respectively, the NMR and X-ray structures of truncated BclXL in complex with BH3 peptides derived from Bad (PDB ID: 1G5J) and Bcl2-interacting mediator (Bim) (PDB ID: 1PQ1) in a multitemplate alignment fashion. A total of 100 structural models were calculated and the structure with the lowest energy, as judged by the MODELLER Objective Function, was selected for further analysis. The structural model was rendered using RIBBONS.[44]

## RESULTS AND DISCUSSION

### BH3 Ligands Recognize BclXL in a Differential Manner

Over the past decade or so, unraveling the specificity of BH3 ligands toward BclXL and other apoptotic repressors has been an area of immense interest. In particular, previous studies have revealed that residues within and flanking the LXXXXD motif account for the specificity of binding of BH3 ligands to apoptotic repressors.[19–31] Importantly, these studies show that in addition to consensus leucine (L0) and aspartate (D+5) within the LXXXXD motif of BH3 peptides (Figure 1b), the hydrophobic residues at the −4, +3, and +7 positions represent interaction "hotspots" that determine the selectivity of molecular recognition by virtue of their ability to align along one face of the amphipathic BH3 α-helix that is accommodated within the binding groove of Bcl2 proteins. In an effort to further build on this work and to understand the ligand specificity of BclXL toward apoptotic activators and effectors, we measured the binding of BclXL to BH3 peptides derived from various Bcl2 proteins using ITC (Figure 2 and Table I).

Our data reveal that while all BH3 ligands are characterized by the presence of the core LXXXXD motif (Figure 1b), residues within and flanking this motif further fortify the BclXL-ligand interaction in a highly rational manner. In particular, the various BH3 ligands of BclXL can be divided into three major classes on the basis of the distinct motifs that they harbor. As noted in Table I, the three major motifs include LXXX[A/S]D (Class I), LXXXGD (Class II), and [R/Q]XLXXXGD (Class III). Of particular note is the observation that the BH3 ligands characterized by these motifs display distinct affinities upon binding to BclXL. Thus, while BH3 ligands harboring the LXXX[A/S]D and [R/Q]XLXXXGD motifs bind to BclXL with submicromolar affinities, those harboring the LXXXGD motif do so with affinities that are between one-to-two orders of magnitude weaker in the micromolar range. This suggests that the presence of a glycine at the fourth position (G+4)—relative to the N-terminal leucine (L0) within the LXXXGD motif (Figure 1b)—mitigates binding, unless the LXXXGD motif also contains arginine/glutamine at the −2 position.

### Energetic Coupling Accounts for High-Affinity Binding of BH3 Ligands to BclXL

Our data presented above provoke the notion that the residues located respectively at the +4 and −2 positions within the LXXX[A/S]D and [R/Q]XLXXXGD motifs are energetically coupled. Simply put, the replacement of alanine/serine at the +4 position is largely compensated by arginine/glutamine at the −2 position and vice versa. To test this hypothesis, we generated various mutant BH3 peptides to probe the effect of appropriate amino acid changes within and flanking the LXXXXD motif and subsequently analyzed their binding to BclXL using ITC in a manner akin to that conducted for wild-type BH3 peptides. As shown in Table II, our analysis reveals that the A+4G substitution within the Puma peptide (Puma_A+4G) harboring the high-affinity LXXX[A/S]D motif results in the loss of binding affinity to BclXL by nearly an order of magnitude, implying that the A+4G replacement within the BH3 ligands harboring the LXXXGD motif indeed accounts for their low-affinity binding to BclXL. This view is further substantiated by the observation that the G+4A substitution within the Harakiri apoptotic activator (Hrk) peptide (Hrk_G+4A) harboring the LXXXGD motif augments its affinity by more than five-folds from micromolar to submicromolar regime. It is noteworthy that such stabilizing effect of

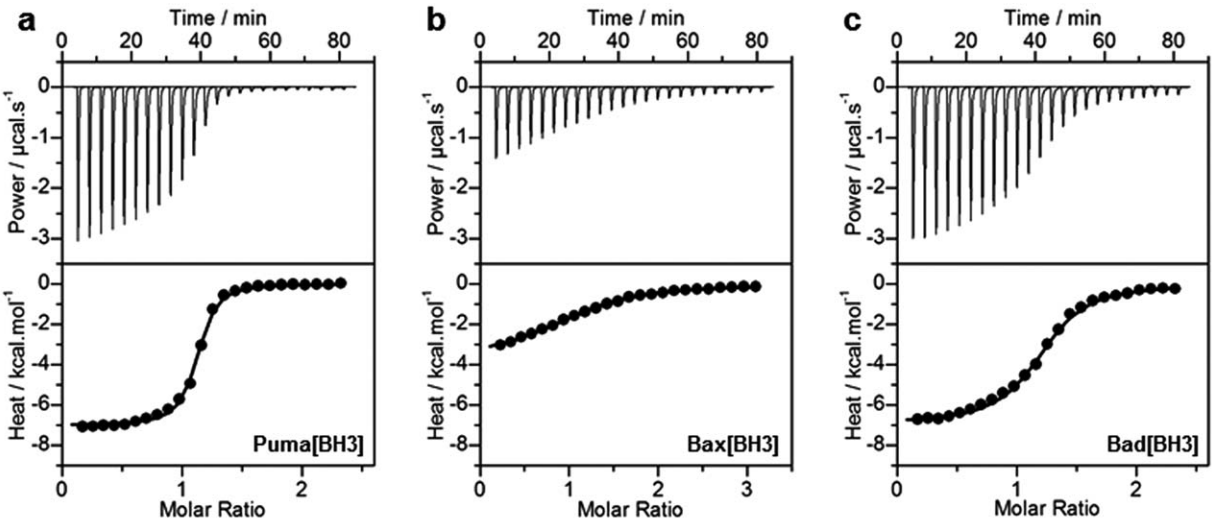


**FIGURE 2** Representative ITC isotherms for the binding of BH3 peptides of Puma (a), Bax (b), and Bad (c) to BclXL in sodium phosphate buffer containing 100 m*M* NaCl at 25°C and pH 7. The upper panels show raw ITC data expressed as change in thermal power with respect to time over the period of titration. In the lower panels, change in molar heat is expressed as a function of molar ratio of each BH3 peptide to BclXL. The solid lines in the lower panels show nonlinear least squares fit of data to a one-site binding model using ORIGIN as described previously.[36,38]

glycine–alanine substitution at the +4 position within the Bim peptide has been previously reported.[25]

Next, to test the notion that the location of an arginine (R-2) or a glutamine (Q-2) at the −2 position restores the loss of binding energy due to the A+4G replacement within the LXXXXD motif, we measured the binding of Bid and Bim peptides respectively harboring the R-2A (Bid_R-2A) and Q-2A (Bim_Q-2A) substitutions to BclXL (Table II). Unsurprisingly, these substitutions mitigate the binding of both of these BH3 peptides harboring the high-affinity [R/Q]XLXXXGD motif to BclXL by several folds. Moreover, the L-2R and A-2Q substitutions within Bcl2-interacting killer (Bik_L-2R) and Hrk (Hrk_A-2Q) peptides harboring the low-affinity LXXXGD motif result in the enhancement of binding affinity to BclXL by close to an order of magnitude. This finding implies that the location of arginine/glutamine at the −2 position

**Table I Thermodynamic Parameters for the Binding of Various Wildtype BH3 Peptides to BclXL in Sodium Phosphate Buffer Containing 100 m*M* NaCl at 25°C and pH 7**

| Peptide | Sequence | $K_d$ (µ*M*) | $\Delta H$ (kcal mol$^{-1}$) | $T\Delta S$ (kcal mol$^{-1}$) | $\Delta G$ (kcal mol$^{-1}$) |
|---|---|---|---|---|---|
| Class I: LXXX[A/S]D motif | | | | | |
| Bmf | QAEVQIARK**L**QCI**AD**QFHRL | 0.20 ± 0.05 | −6.67 ± 0.22 | +2.50 ± 0.07 | −9.17 ± 0.15 |
| Puma | QWAREIGAQ**L**RRM**AD**DLNAQ | 0.22 ± 0.05 | −6.88 ± 0.16 | +2.23 ± 0.03 | −9.11 ± 0.14 |
| Bad | WAAQRYGRE**L**RRM**SD**EFVDS | 0.41 ± 0.15 | −7.00 ± 0.14 | +1.74 ± 0.09 | −8.74 ± 0.23 |
| Class II: LXXXGD motif | | | | | |
| Hrk | SAAQLTAAR**L**KAL**GD**ELHQR | 4.69 ± 1.21 | −3.32 ± 0.06 | +3.97 ± 0.21 | −7.29 ± 0.15 |
| Bax | ASTKKLSES**L**KRI**GD**ELDSN | 6.35 ± 1.13 | −3.50 ± 0.04 | +3.59 ± 0.07 | −7.10 ± 0.11 |
| Bik | EGSDALALR**L**ACI**GD**EMDVS | 17.49 ± 2.98 | −2.68 ± 0.09 | +3.81 ± 0.19 | −6.50 ± 0.11 |
| Noxa | ELEVECATQ**L**RRF**GD**KLNFR | 26.01 ± 6.05 | −3.21 ± 0.12 | +3.06 ± 0.25 | −6.26 ± 0.14 |
| Class III: [R/Q]XLXXXGD motif | | | | | |
| Bid | DIIRNIA**RH**L**A**QV**GD**SMDRS | 0.35 ± 0.07 | −7.18 ± 0.27 | +1.64 ± 0.15 | −8.82 ± 0.12 |
| Bim | RPEIWIA**QE**L**R**RI**GD**EFNAY | 0.65 ± 0.17 | −2.25 ± 0.07 | +6.21 ± 0.08 | −8.46 ± 0.15 |
| Bak | STMGQVG**RQ**L**A**II**GD**DINRR | 0.47 ± 0.09 | −7.58 ± 0.18 | +1.07 ± 0.06 | −8.65 ± 0.12 |

Note that the BH3 peptides are divided into three classes on the basis of the consensus motif that they harbor. Consensus residues within each motif are colored red. All parameters were obtained from ITC measurements. Errors were calculated from at least three independent measurements to one standard deviation. Noxa, Phorbol-induced protein 1.

**Table II Thermodynamic Parameters for the Binding of Various Mutant BH3 Peptides to BclXL in Sodium Phosphate Buffer Containing 100 m*M* NaCl at 25°C and pH 7**

| Peptide | Sequence | $K_d$ ($\mu M$) | $\Delta H$ (kcal mol$^{-1}$) | $T\Delta S$ (kcal mol$^{-1}$) | $\Delta G$ (kcal mol$^{-1}$) |
|---|---|---|---|---|---|
| Puma_A+4G | QWAREIGAQ**L**RRM**GD**DLNAQ | 1.80 ± 0.46 | −6.49 ± 0.09 | +1.37 ± 0.05 | −7.86 ± 0.15 |
| Hrk_G+4A | SAAQLTAAR**L**KAL**AD**ELHQR | 0.81 ± 0.17 | −1.09 ± 0.04 | +7.23 ± 0.08 | −8.33 ± 0.13 |
| Bid_R-2A | DIIRNIA**AH**L**A**QVG**D**SMDRS | 1.59 ± 0.27 | −6.49 ± 0.11 | +1.43 ± 0.01 | −7.92 ± 0.12 |
| Bim_Q-2A | RPEIWIA**AE**L**A**RIG**D**EFNAY | 1.60 ± 0.35 | −0.95 ± 0.02 | +6.97 ± 0.14 | −7.92 ± 0.13 |
| Bik_L-2R | EGSDALA**RR**L**A**CIG**D**EMDVS | 2.11 ± 0.55 | −4.44 ± 0.15 | +3.33 ± 0.01 | −7.76 ± 0.16 |
| Hrk_A-2Q | SAAQLTA**QR**L**A**LG**D**ELHQR | 0.78 ± 0.16 | −2.80 ± 0.08 | +5.54 ± 0.05 | −8.34 ± 0.12 |
| Bad_R-2A | WAAQRYG**AE**L**A**RMS**D**EFVDS | 0.58 ± 0.13 | −3.72 ± 0.16 | +4.80 ± 0.03 | −8.52 ± 0.13 |
| Bad_AA | WAAQRYG**AE**L**A**RM**AD**EFVDS | 0.31 ± 0.05 | −5.06 ± 0.13 | +3.84 ± 0.03 | −8.90 ± 0.10 |
| Bad_AG | WAAQRYG**AE**L**A**RM**GD**EFVDS | 1.80 ± 0.37 | −3.09 ± 0.08 | +4.77 ± 0.04 | −7.85 ± 0.12 |
| Bmf_R-2A | QAEVQIA**AK**L**A**QCIA**D**QFHRL | 0.32 ± 0.08 | −5.73 ± 0.20 | +3.15 ± 0.04 | −8.88 ± 0.16 |
| Bmf_A+4G | QAEVQIARK**L**A**GD**QFHRL | 0.43 ± 0.14 | −6.14 ± 0.13 | +2.57 ± 0.07 | −8.71 ± 0.20 |
| Bmf_AG | QAEVQIA**AK**L**A**QCI**GD**QFHRL | 6.53 ± 1.43 | −3.65 ± 0.17 | +3.44 ± 0.03 | −7.09 ± 0.13 |

Note that the absolutely conserved leucine and aspartate residues within the core LXXXXD motif shared by all BH3 peptides are colored red, while the mutated residues within and flanking this motif are shown in blue for clarity. The nomenclature used for the relative positions of various residues is as described in Figure 1b. All parameters were obtained from ITC measurements. Errors were calculated from at least three independent measurements to one standard deviation.

promotes the binding of BH3 ligands harboring the [R/Q]XLXXXGD motif with high affinity. Notably, of all the BH3 ligands analyzed here, Bad is the only one that contains a serine residue at the +4 position (S+4) within the LXXXXD motif in lieu of an alanine or a glycine. To test whether a serine can substitute for an alanine (A+4) or whether it mimics glycine (G+4) at the +4 position, we introduced the R-2A substitution into Bad peptide (Bad_R-2A) harboring the RXLXXXSD motif and measured its binding to BclXL (Table II). Our data show that the R-2A substitution has negligible effect on the binding affinity of Bad peptide, implying that the S+4 residue behaves in a manner akin to A+4 in lieu of G+4. To further test this notion, we also introduced R-2A/S+4A (Bad_AA) and R-2A/S+4G (Bad_AG) double substitutions into Bad peptide and analyzed their binding to BclXL. Consistent with our hypothesis, while the binding of Bad_AA peptide (AXLXX-X[A/S]D) to BclXL is accompanied by an affinity similar to that observed for the binding of wildtype Bad peptide, the Bad_AG peptide (AXLXXXGD) displays low-affinity binding to BclXL by about five-folds. This further corroborates the view that the energetic contribution of S+4 residue is similar to that of A+4 instead of G+4 within the LXXXXD motif.

Finally, to directly test the notion that the residues located respectively at the +4 and −2 positions within the LXXX[A/S]D and [R/Q]XLXXXGD motifs are energetically coupled, we introduced the R-2A [Bcl2-modifying factor (Bmf)] (Bmf_R-2A) and A+4G (Bmf_A+G) single substitutions along with the R-2A/A+4G double-substitution (Bmf_AG) into Bmf peptide and analyzed their binding to BclXL (Table II). Consistent with our data presented above, while the binding of Bmf_R-2A and Bmf_A+4G single-mutant peptides to BclXL results in the cumulative loss of binding energy of less than 1 kcal/mol relative to the wildtype Bmf peptide, the binding of Bmf_AG double-mutant peptide encounters the loss of more than 2 kcal/mol of binding energy. This unequivocally demonstrates that the loss of at least an extra 1 kcal/mol of free energy accompanying the binding of double-mutant Bmf peptide relative to composite effect of single-mutant Bmf peptides represents the contribution of coupling energy arising from energetic coupling of residues located, respectively, at the +4 and −2 positions within the LXXX[A/S]D and [R/Q]XLXXXGD motifs.

## Differential Binding of BH3 Ligands to BclXL Poorly Correlates with the Extent of Surface Burial

To understand the contribution of polar and apolar residues in driving the BclXL-ligand interactions, we next measured the dependence of enthalpic change ($\Delta H$) associated with the binding of various BH3 peptides to BclXL on temperature (Figure 3). Importantly, the temperature-dependence of $\Delta H$ is related to the change in heat capacity ($\Delta C_p$) by Kirchhoff's relationship $\Delta C_p = d(\Delta H)/dT$, where $T$ denotes temperature. Accordingly, $\Delta C_p$ accompanying the binding of various BH3 peptides to BclXL was determined from the corresponding slopes of $\Delta H$–$T$ plots (Figure 3 and Table III). It is noteworthy that a negative value of $\Delta C_p$ was observed across-the-board, implying that the binding of all BH3 peptides to BclXL is concomitant with the burial of predominantly apolar residues over polar groups. However, there appears to be a little

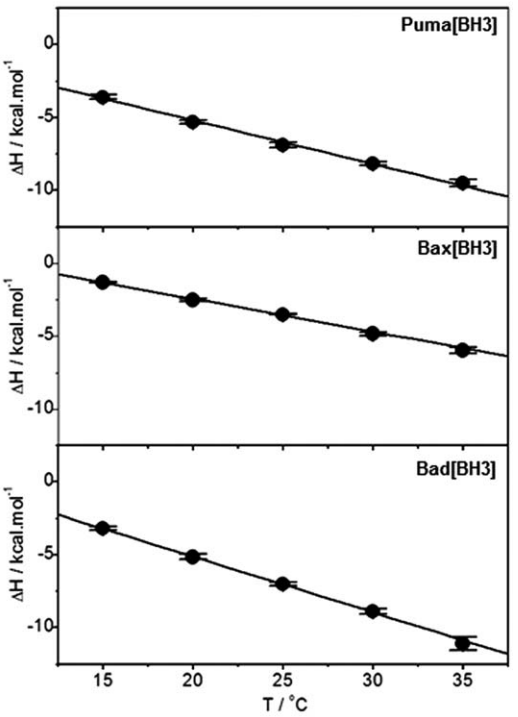


**FIGURE 3** Dependence of enthalpy ($\Delta H$) on temperature ($T$) for the binding of BH3 peptides of Puma, Bax, and Bad to BclXL in sodium phosphate buffer containing 100 m*M* NaCl at pH 7. The solid lines through the data points represent linear fits. Error bars were calculated from at least three independent measurements to one standard deviation.

correlation between $\Delta C_p$ and the free energy ($\Delta G$) of binding. Thus, for example, while $\Delta C_p$ accompanying the binding of high-affinity ligand such as Puma is −304 cal/mol/K, low-affinity ligand such as Hrk experiences only a slightly smaller $\Delta C_p$ of −276 cal/mol/K. On the other hand, while both high-affinity ligands such as Bid and Bad bind to BclXL with similar affinities, the $\Delta C_p$ associated with the binding of Bad (−389 cal/mol/K) is more than twofold greater than that of Bid (−172 cal/mol/K).

To quantify how such differential changes in $\Delta C_p$ may reflect the extent of burial of polar and apolar surfaces upon the binding of various BH3 ligands to BclXL, we also calculated the corresponding changes in SASA using empirically derived Eqs. (3) and (4).[39–42] As noted in Table III, the change in apolar SASA ($\Delta SASA_{apolar}$) is on average about 50% greater than the corresponding change in polar SASA ($\Delta SASA_{polar}$) for the binding of each BH3 peptide to BclXL. This implies that the hydrophobic forces play a dominant role in driving BclXL-ligand interactions.

## Hydrophobic and Electrostatic Interactions Contribute Differentially to the Binding of Various BH3 Ligands to BclXL

The fact that the differential binding of BH3 ligands to BclXL poorly correlates with the extent of surface area burial, as measured by changes in heat capacity change, strongly suggests that hydrophobic residues and salt bridges play an intricate role in mediating the BclXL-ligand interactions. In an attempt to further elucidate such interplay between these forces, we next measured the effect of increasing NaCl concentration on the binding of BH3 peptides to BclXL (Figure 4). Our data reveal that salt modulates the binding of high-affinity Class I (LXXX[A/S]D) and Class III ([R/Q]XLXXXGD) ligands to BclXL in a distinct manner from that observed for low-affinity Class II (LXXXGD) ligands. Thus, while increasing salt

**Table III ΔSASA Values Determined from Thermodynamic Parameters for the Binding of Various Wildtype BH3 Peptides to BclXL in Sodium Phosphate Buffer Containing 100 m*M* NaCl at pH 7**

| Peptide | Sequence | $\Delta H_{60}$ (kcal mol$^{-1}$) | $\Delta C_p$ (cal mol$^{-1}$ K$^{-1}$) | $\Delta SASA_{polar}$ (Å$^2$) | $\Delta SASA_{apolar}$ (Å$^2$) | $\Delta SASA_{total}$ (Å$^2$) |
|---|---|---|---|---|---|---|
| Class I: LXXX[A/S]D motif | | | | | | |
| Puma | QWAREIGAQ**L**RRM**AD**DLNAQ | −17.24 ± 0.25 | −304 ± 5 | −914 ± 12 | −1350 ± 14 | −2264 ± 26 |
| Bmf | QAEVQIARK**L**QCI**AD**QFHRL | −18.78 ± 0.38 | −356 ± 4 | −1019 ± 18 | −1558 ± 21 | −2578 ± 39 |
| Bad | WAAQRYGRE**L**RRM**SD**EFVDS | −20.73 ± 0.64 | −389 ± 12 | −1122 ± 35 | −1708 ± 53 | −2829 ± 88 |
| Class II: LXXXGD motif | | | | | | |
| Bax | ASTKKLSES**L**KRI**GD**ELDSN | −11.81 ± 0.36 | −234 ± 7 | −650 ± 21 | −1014 ± 34 | −1664 ± 54 |
| Hrk | SAAQLTAAR**L**KAL**GD**ELHQR | −12.93 ± 0.16 | −276 ± 3 | −731 ± 8 | −1183 ± 12 | −1914 ± 21 |
| Bik | EGSDALALR**L**ACI**GD**EMDVS | −8.43 ± 0.34 | −164 ± 6 | −461 ± 18 | −713 ± 28 | −1174 ± 46 |
| Noxa | ELEVECATQ**L**RRF**GD**KLNFR | −9.19 ± 0.07 | −168 ± 4 | −493 ± 6 | −741 ± 16 | −1233 ± 23 |
| Class III: [R/Q]XLXXXGD motif | | | | | | |
| Bid | DIIRNIA**R**H**L**AQV**GD**SMDRS | −13.35 ± 0.34 | −172 ± 4 | −647 ± 17 | −819 ± 23 | −1466 ± 40 |
| Bim | RPEIWIA**Q**E**L**RRI**GD**EFNAY | −8.50 ± 0.29 | −175 ± 4 | −475 ± 15 | −755 ± 19 | −1229 ± 35 |
| Bak | STMGQVG**R**Q**L**AII**GD**DINRR | −16.64 ± 0.33 | −261 ± 4 | −851 ± 16 | −1188 ± 20 | −2039 ± 37 |

Errors were calculated from at least three independent measurements to one standard deviation. Noxa, Phorbol-induced protein 1.

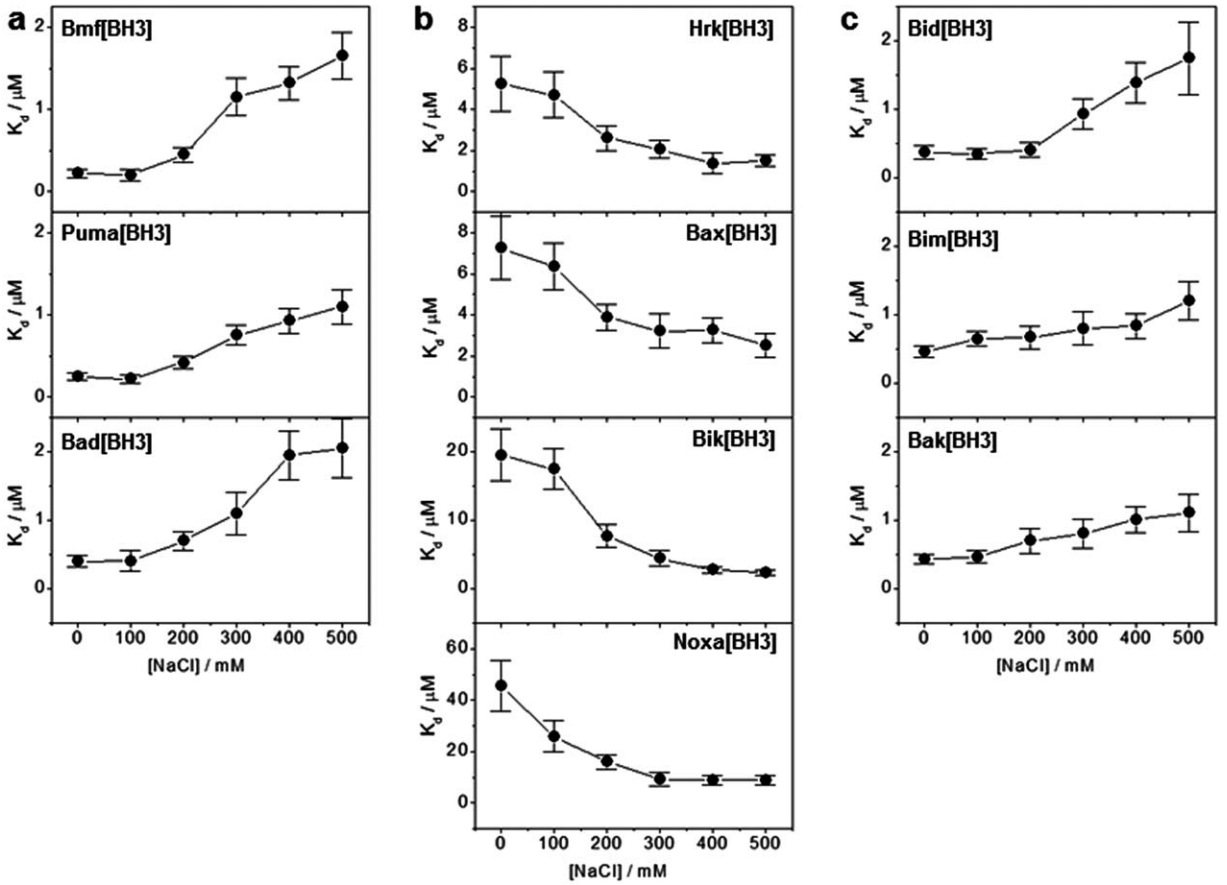


**FIGURE 4** Effect of NaCl concentration on the binding, as measured by the binding constant ($K_d$), of various BH3 peptides harboring LXXX[A/S]D (a), LXXXGD (b), and [R/Q]XLXXXGD (c) motifs to BclXL in sodium phosphate buffer at 25°C and pH 7. Note that the solid lines are used to connect various data points for clarity. Error bars were calculated from at least three independent measurements to one standard deviation.

concentration from 0 to 500 m*M* is concomitant with a reduction in the binding of Class I and III ligands to BclXL from submicromolar to low micromolar range (Figures 4a and 4c), Class II ligands experience an increase in binding affinity by up to several folds over the same salt concentration range (Figure 4b). This strongly suggests that while hydrophobic residues likely dominate ionic interactions in driving the binding of Class II ligands to BclXL, the converse applies in the case of Class I and III ligands. While it is clearly beyond the scope of this study, these data warrant further investigation into the differential role of specific charged and hydrophobic residues in driving BclXL-ligand interactions.

## CONCLUSIONS

While it is well understood that the various BH3 ligands recognize apoptotic repressors such as BclXL with distinct affinities,[19–31] our data presented above lend new insights into the molecular determinants of their specificity and recognition. In particular, our analysis suggests that the various proapoptotic BH3 ligands of BclXL can be all dissected into three distinct classes harboring the LXXX[A/S]D (Class I), LXXXGD (Class II) and [R/Q]XLXXXGD (Class III) motifs on the basis of their sequence and binding characteristics. Thus, while Class I and III ligands appear to recognize BclXL with high affinity in the submicromolar range, Class II ligands afford weak interactions. While our study suggests that the differential binding of various BH3 ligands to BclXL can be rationalized in terms of three distinct motifs that they harbor, it should however be borne in mind that additional residues within and flanking the core LXXXXD motif are also likely to participate in key intermolecular contacts, thereby adding another layer of complexity to understanding the differences in the binding of BH3 ligands to BclXL.

In particular, the role of nonconsensus residues within and flanking the LXXX[A/S]D, LXXXGD and [R/Q]XLXXXGD motifs is likely to be context-dependent and this could further blur the rather simple picture presented here. It is also noteworthy that while the distinction between LXXX[A/S]D (Class I) and [R/Q]XLXXXGD (Class III) motifs is poor, it was nonetheless necessary to emphasize the fact that the molecular origin underlying high-affinity binding of these two motifs is quite distinct. Thus, while the LXXX[A/S]D motif would achieve high-affinity binding by virtue of the presence of an alanine/serine at the +4 position, the [R/Q]XLXXXGD motif would do so via the presence of an arginine/glutamine at the −2 position owing to the fact that these residues are energetically coupled. On the other hand, the choice to place both the glutamine and arginine at the −2 position in the same category was largely based on the fact that the Bim peptide harboring a glutamine at the −2 position binds to BclXL with an affinity that is virtually indistinguishable from those observed for the binding of Bid and Bak peptides, both of which contain an arginine at the −2 position. Nonetheless, we acknowledge that such merger is somewhat arbitrary and further work is warranted to shed new light into the role of specific residues not only at the −2 position but also at other positions within the LXXXXD motif.

In short, our study advances our understanding of the binding specificity of BH3 ligands to BclXL and other apoptotic repressors. Given that numerous efforts have been directed toward the development of structural mimetics of BH3 peptides that could target BclXL and other apoptotic repressors with high selectivity over the past decade or so,[45–52] the importance of our current work on the design of such novel anticancer inhibitors cannot be overemphasized.

## REFERENCES


1. Adams, J. M.; Cory, S. Science 1998, 281, 1322–1326.
2. Gross, A.; McDonnell, J. M.; Korsmeyer, S. J. Genes Dev 1999, 13, 1899–1911.
3. Korsmeyer, S. J. Cancer Res 1999, 59, 1693s–1700s.
4. Kuwana, T.; Newmeyer, D. D. Curr Opin Cell Biol 2003, 15, 691–699.
5. Dewson, G.; Kluck, R. M. J Cell Sci 2009, 122, 2801–2808.
6. Chipuk, J. E.; Moldoveanu, T.; Llambi, F.; Parsons, M. J.; Green, D. R. Mol Cell 2010, 37, 299–310.
7. Dejean, L. M.; Ryu, S. Y.; Martinez-Caballero, S.; Teijido, O.; Peixoto, P. M.; Kinnally, K. W. Biochim Biophys Acta 2010, 1797, 1231–1238.
8. Martinou, J. C.; Youle, R. J. Dev Cell 2011, 21, 92–101.
9. Chipuk, J. E.; Fisher, J. C.; Dillon, C. P.; Kriwacki, R. W.; Kuwana, T.; Green, D. R. Proc Natl Acad Sci USA 2008, 105, 20327–20332.
10. Chipuk, J. E.; Green, D. R. Trends Cell Biol 2008, 18, 157–164.
11. van der Goot, F. G.; Gonzalez-Manas, J. M.; Lakey, J. H.; Pattus, F. Nature 1991, 354, 408–410.
12. London, E. Biochim Biophys Acta 1992, 1113, 25–51.
13. Lakey, J. H.; van der Goot, F. G.; Pattus, F. Toxicology 1994, 87, 85–108.
14. Schendel, S. L.; Montal, M.; Reed, J. C. Cell Death Differ 1998, 5, 372–380.
15. Zakharov, S. D.; Cramer, W. A. Biochim Biophys Acta 2002, 1565, 333–346.
16. Del Bufalo, D.; Biroccio, A.; Leonetti, C.; Zupi, G. FASEB J 1997, 11, 947–953.
17. Espana, L.; Fernandez, Y.; Rubio, N.; Torregrosa, A.; Blanco, J.; Sierra, A. Breast Cancer Res Treat 2004, 87, 33–44.
18. Placzek, W. J.; Wei, J.; Kitada, S.; Zhai, D.; Reed, J. C.; Pellecchia, M. Cell Death Dis 2010, 1, e40.
19. Sattler, M.; Liang, H.; Nettesheim, D.; Meadows, R. P.; Harlan, J. E.; Eberstadt, M.; Yoon, H. S.; Shuker, S. B.; Chang, B. S.; Minn, A. J.; Thompson, C. B.; Fesik, S. W. Science 1997, 275, 983–986.
20. Huang, D. C.; Strasser, A. Cell 2000, 103, 839–842.
21. Petros, A. M.; Nettesheim, D. G.; Wang, Y.; Olejniczak, E. T.; Meadows, R. P.; Mack, J.; Swift, K.; Matayoshi, E. D.; Zhang, H.; Thompson, C. B.; Fesik, S. W. Protein Sci 2000, 9, 2528–2534.
22. Liu, X.; Dai, S.; Zhu, Y.; Marrack, P.; Kappler, J. W. Immunity 2003, 19, 341–352.
23. Petros, A. M.; Olejniczak, E. T.; Fesik, S. W. Biochim Biophys Acta 2004, 1644, 83–94.
24. Lee, E. F.; Czabotar, P. E.; Smith, B. J.; Deshayes, K.; Zobel, K.; Colman, P. M.; Fairlie, W. D. Cell Death Differ 2007, 14, 1711–1713.
25. Boersma, M. D.; Sadowsky, J. D.; Tomita, Y. A.; Gellman, S. H. Protein Sci 2008, 17, 1232–1240.
26. Noble, C. G.; Dong, J. M.; Manser, E.; Song, H. J Biol Chem 2008, 283, 26274–26282.
27. Moroy, G.; Martin, E.; Dejaegere, A.; Stote, R. H. J Biol Chem 2009, 284, 17499–17511.
28. Yao, Y.; Bobkov, A. A.; Plesniak, L. A.; Marassi, F. M. Biochemistry 2009, 48, 8704–8711.
29. Dutta, S.; Gulla, S.; Chen, T. S.; Fire, E.; Grant, R. A.; Keating, A. E. J Mol Biol 2010, 398, 747–762.
30. Ku, B.; Liang, C.; Jung, J. U.; Oh, B. H. Cell Res 2011, 21, 627–641.
31. London, N.; Gulla, S.; Keating, A. E.; Schueler-Furman, O. Biochemistry 2012, 51, 5841–5850.
32. Krajewski, S.; Tanaka, S.; Takayama, S.; Schibler, M. J.; Fenton, W.; Reed, J. C. Cancer Res 1993, 53, 4701–4714.
33. Gonzalez-Garcia, M.; Perez-Ballestero, R.; Ding, L.; Duan, L.; Boise, L. H.; Thompson, C. B.; Nunez, G. Development 1994, 120, 3033–3042.
34. Zha, H.; Fisk, H. A.; Yaffe, M. P.; Mahajan, N.; Herman, B.; Reed, J. C. Mol Cell Biol 1996, 16, 6494–6508.
35. Bhat, V.; Kurouski, D.; Olenick, M. B.; McDonald, C. B.; Mikles, D. C.; Deegan, B. J.; Seldeen, K. L.; Lednev, I. K.; Farooq, A. Arch Biochem Biophys 2012, 528, 32–44.
36. Bhat, V.; McDonald, C. B.; Mikles, D. C.; Deegan, B. J.; Seldeen, K. L.; Bates, M. L.; Farooq, A. J Mol Biol 2012, 416, 57–77.
37. Gasteiger, E.; Hoogland, C.; Gattiker, A.; Duvaud, S.; Wilkins, M. R.; Appel, R. D.; Bairoch, A. In The Proteomics Protocols Handbook; Walker, J. M., Ed.; Humana Press: Totowa, New Jersey, 2005; pp 571–607.
38. Wiseman, T.; Williston, S.; Brandts, J. F.; Lin, L. N. Anal Biochem 1989, 179, 131–137.

39. Murphy, K. P.; Freire, E. Adv Protein Chem 1992, 43, 313–361.
40. Spolar, R. S.; Record, M.T., Jr. Science 1994, 263, 777–784.
41. Xie, D.; Freire, E. Proteins 1994, 19, 291–301.
42. Edgcomb, S. P.; Murphy, K. P. Curr Opin Biotechnol 2000, 11, 62–66.
43. Marti-Renom, M. A.; Stuart, A. C.; Fiser, A.; Sanchez, R.; Melo, F.; Sali, A. Annu Rev Biophys Biomol Struct 2000, 29, 291–325.
44. Carson, M. J Appl Crystallogr 1991, 24, 958–961.
45. Walensky, L. D.; Kung, A. L.; Escher, I.; Malia, T. J.; Barbuto, S.; Wright, R. D.; Wagner, G.; Verdine, G. L.; Korsmeyer, S. J. Science 2004, 305, 1466–1470.
46. Sadowsky, J. D.; Schmitt, M. A.; Lee, H. S.; Umezawa, N.; Wang, S.; Tomita, Y.; Gellman, S. H. J Am Chem Soc 2005, 127, 11966–11968.
47. Walensky, L. D.; Pitter, K.; Morash, J.; Oh, K. J.; Barbuto, S.; Fisher, J.; Smith, E.; Verdine, G. L.; Korsmeyer, S. J Mol Cell 2006, 24, 199–210.
48. Sadowsky, J. D.; Fairlie, W. D.; Hadley, E. B.; Lee, H. S.; Umezawa, N.; Nikolovska-Coleska, Z.; Wang, S.; Huang, D. C.; Tomita, Y.; Gellman, S. H. J Am Chem Soc 2007, 129, 139–154.
49. Sadowsky, J. D.; Murray, J. K.; Tomita, Y.; Gellman, S. H. Chembiochem 2007, 8, 903–916.
50. Horne, W. S.; Boersma, M. D.; Windsor, M. A.; Gellman, S. H. Angew Chem Int Ed Engl 2008, 47, 2853–2856.
51. Lee, E. F.; Smith, B. J.; Horne, W. S.; Mayer, K. N.; Evangelista, M.; Colman, P. M.; Gellman, S. H.; Fairlie, W. D. Chembiochem 2011, 12, 2025–2032.
52. Boersma, M. D.; Haase, H. S.; Peterson-Kaufman, K. J.; Lee, E. F.; Clarke, O. B.; Colman, P. M.; Smith, B. J.; Horne, W. S.; Fairlie, W. D.; Gellman, S. H. J Am Chem Soc 2012, 134, 315–323.

*Reviewing Editor: Alfred Wittinghofer*